Adaptive Finite-Time Trajectory Tracking Control of Autonomous Vehicles That Experience Disturbances and Actuator Saturation

***Abstract*—This article presents a finite-time tracking control scheme for autonomous vehicles. Trajectory tracking is difficult to control due to dynamic couplings and various disturbances and uncertainties. To cope with a lumped disturbance, a fuzzy logic system is designed. In particular, a novel adaptive algorithm is constructed to adjust the gain online, and it works well even without the prior information of the lumped disturbance bounds. An auxiliary system with a simple structure is built to tackle the actuator saturation. Moreover, the proposed control method can guarantee finite-time error convergence, chattering elimination, and strong robustness. Experiment results are presented to show the effectiveness of the control schemes.**

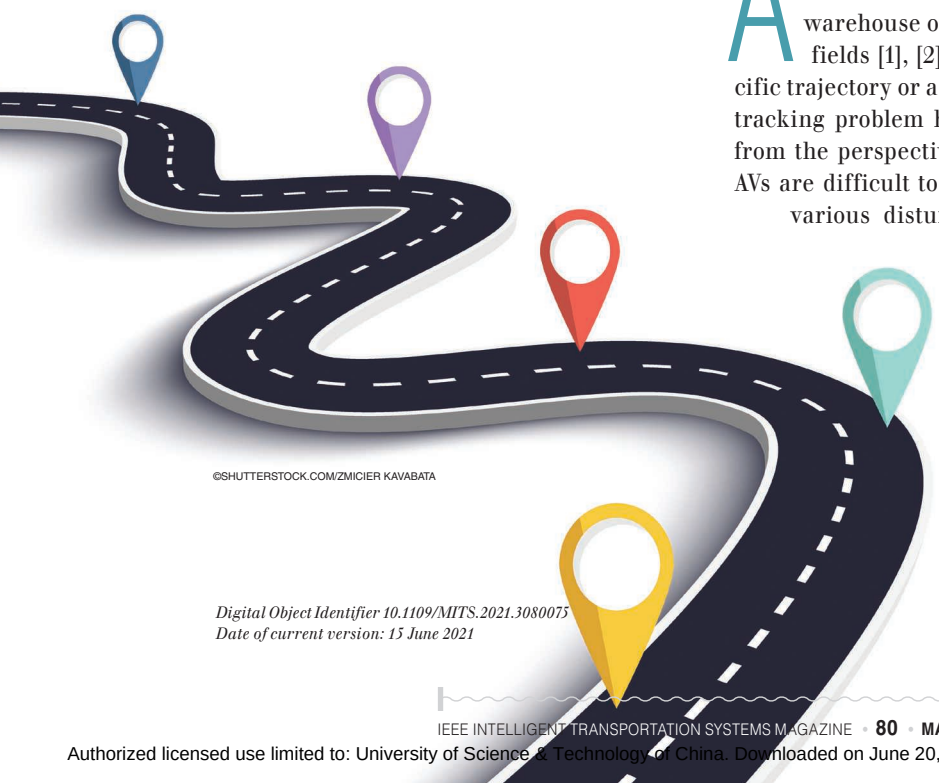

Digital Object Identifier 10.1109/MITS.2021.3080075
Date of current version: 15 June 2021

Autonomous vehicles (AVs) have attracted significant research interest in areas including mine clearance, warehouse operations, planetary exploration, and other fields [1], [2]. AVs are often tasked with tracking a specific trajectory or a moving virtual target. Thus, the trajectory tracking problem has been widely studied [3], [4]. However, from the perspective of theoretical and practical challenges, AVs are difficult to control because of dynamic coupling and various disturbances in modeling processes and real operations [5]. To deal with the difficulties, several control laws have been proposed, which can generally be divided into two categories: 1) pure kinematic control input and 2) kinematic and dynamic hybrid control inputs.

The kinematic model is constructed to generate appropriate velocity control signals to minimize the accumulated tracking error between the actual and the reference trajectories. Major kinematic control approaches consist of backstepping [6], dynamic feedback

1939-1390/22©2022IEEE

Hongbo Gao and Zhen Kan
Are with the University of Science and Technology of China, Hefei, 230026, China.
Email: ghb48@ustc.edu.cn; zkan@ustc.edu.cn

Fei Chen
Is with the Chinese University of Hong Kong, Hong Kong, 999077, China. Email: f.chen@ieee.org

Zhengyuan Hao* and Xi He
Are with the University of Science and Technology of China, Hefei, 230026, China.
Email: zyhao@mail.ustc.edu.cn; hexi88@mail.ustc.edu.cn

Hang Su
Is with Politecnico di Milano, Milano, 20133, Italy.
Email: hang.su@polimi.it

Keqiang Li
Is with Tsinghua University, Beijing, 100084, China.
Email: likq@tsinghua.edu.cn

linearization [7], and velocity scheduling [8], to name just a few. In [6], Jiang and Nijmeijer achieved local and global trajectory tracking goals with exponential convergence. In [7], Oriolo et al. solved the tracking problem and the posture stabilization of vehicle systems by means of dynamic feedback linearization. In [8], Buccieri et al. proposed a higher-dimensional state extension to eliminate the adverse impact of disturbances on a vehicle body's rotational axis to improve the performance of dynamic feedback linearization. Although the methods in [6]–[8] provide rigorous stability analysis, they are based on an ideal assumption of "perfect velocity tracking," which is not practical. Besides, the performance of pure kinematic controllers is limited since the dynamic model is ignored.

To overcome the shortcomings of pure kinematic controllers, several approaches have been proposed based on the integration of kinematic and dynamic models. Many control algorithms for trajectory tracking have been developed, such as adaptive control [9], [10], neural networks (NNs) [11], fuzzy logic systems (FLSs) [12], and so on. Park et al. proposed a leader–follower-based adaptive control scheme to achieve collision avoidance when velocity signals are not available [9]. In [11], to avoid manual weight adjustment, a learning-based control policy was introduced using a three-layer NN. Owing to the capability of conveying human knowledge, FLSs, as an alternative intelligent policy, can handle unknown processes and provide excellent performance in practical applications [12], [13]. In [12], a fuzzy sliding mode control (SMC) was presented to tackle uncertainties through chattering avoidance. Despite the advantages of these methods, few existing works consider the finite-time error convergence of AVs.

With the development of control theory and the growing demand for the finite-time tracking of vehicle systems, the finite-time controller has become a major research area [14]. Popular methodologies for finite-time controllers include SMC [15], finite-time observers [16], adding a power integrator [17], and so on. Because SMC has the significant characteristics of a simple control structure and strong robustness, it is an effective and widely used technical strategy. The authors of [18] showed the distinctive merit of the NN sign function in achieving more than finite-time stability for an SMC system, and singularity-free SMC laws were designed and demonstrated to achieve simultaneous-arrival-to-origin convergence. Recently, terminal SMC (TSMC) was proposed, which can provide a predefined finite settling time. Based on a discrete-time point of view, a discrete-time TSMC was presented in [19]. However, the conventional TSMC faces the singularity problem, and its convergence speed is relatively slow compared to traditional SMC when the system state is far from equilibrium.

To solve these issues, a new SMC, called the *nonsingular, fast terminal SMC* (*NFTSMC*), was presented and applied in [20] and [21]. Nevertheless, as a common challenge, it is hard to avoid undesired chattering. The most common method that uses a boundary layer technique [22]

*Corresponding author

AVs are often tasked with tracking a specific trajectory or a moving virtual target. Thus, the trajectory tracking problem has been widely studied.

or a hyperbolic tangent function [23] is to replace the discontinuous signum function in the switching controller. However, these solutions have the following shortcomings: 1) the stability inside the boundary layer fails to be ensured and 2) the poor selection of the width of the boundary layer is prone to system instability. Therefore, in this article, our intention is to design a fast finite-time control signal without sacrificing robust performance.

Alternatively, vehicle systems with actuator saturation are common in practice. However, most of the previous research ignores this issue. To guarantee human safety and satisfy special operational requirements, actuator saturation should be taken into consideration [24], [25]. The research results regarding actuator saturation mainly focus on two aspects, i.e., the small-gain controller to reduce the input amplitude [26] and the use of saturation functions to compensate the saturation region [27]. In [26], Sun et al. proposed a quasi-proportional–integral–derivative controller using the properties of the hyperbolic tangent function to eliminate the effect of input saturation. The work in [27] presented an NN-based approach to deal with uncertainty and actuator saturation. From the perspective of controller design and practical application, the solution to actuator saturation is still largely unknown.

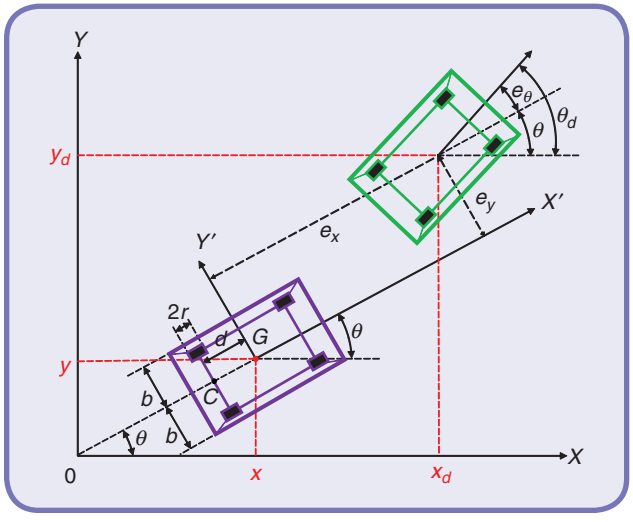

FIG 1 The general dynamics model of an AV.

Motivated by the preceding discussion, we design a saturated, adaptive fuzzy NFTSMC (SAFNFTSMC) scheme to solve the tracking control problem for AVs in the presence of external disturbances and to resolve the issue of actuator saturation and thus achieve the objectives of fast finite-time error convergence, chattering avoidance, and online gain adjustment. The main contributions of this article are as follows:

1) An FLS is designed, and a novel adaptive algorithm is constructed to adjust the gain online, which can work well without the prior information of the lumped disturbance bounds. Therefore, the lumped disturbance problem can be solved.
2) An auxiliary system with a simple structure is built. Thus, the actuator saturation problem can be solved. An SAFNFTSMC is designed to solve the tracking control problem for AVs.
3) The proposed control method is adopted to guarantee finite-time error convergence, chattering elimination, and strong robustness.

Notations

The following notations are used. For a vector $x = [x_1, \ldots, x_n]^T$, the vector powers are designed as $x^\alpha = [x_1^\alpha, \ldots, x_n^\alpha]^T \in \mathbb{R}^n$ and $|x|^\alpha = \text{diag}\{|x_1|^\alpha, \ldots, |x_n|^\alpha\} \in \mathbb{R}^{n\times n}$. To improve readability, $\text{sign}(x)^\alpha \in \mathbb{R}^n$ is defined as $\text{sign}(x)^\alpha = |x|^\alpha \text{sign}(x) = [|x_1|^\alpha \text{sign}(x_1), \ldots, |x_n|^\alpha \text{sign}(x_n)]^T$, and we obtain $(d/dt)(\text{sign}(x)^\alpha) = \alpha |x|^{\alpha-1}\dot{x}$, with $\alpha \geq 1$. Additionally, sign $(\cdot)$, diag$\{\cdot\}$, and $\|\cdot\|$ represent the signum function, diagonal matrix, and Euclidean norm, respectively.

Models and Problem Formulation

AV Model

As shown in Figure 1, the general dynamics model of an AV can be described as follows [28], [29]:

$$C(q)\ddot{q} + B(q,\dot{q})\dot{q} + F(\dot{q}) + d = E(q)\tau - A^T(q)\lambda, \quad (1)$$

$$\dot{q} = J(q)\eta, \quad (2)$$

where $q = [x, y, \theta]^T$, $J(q)$ is a Jacobian matrix, $\eta = [v, w]^T$, and $\tau = [\tau_r, \tau_l]^T$ denotes the input torques generated by the left and right motors. The definitions of other system matrices are provided in [29] and [30]. (See Table 1 for additional information.) Derive equation (2) about time, then get $\ddot{q} = J_q\dot{\eta} + (J_q \odot \dot{q})\eta$, in which J_q indicates the partial derivative of matrix $J(q)$ with respect to parament q and the symbol $\odot$ represents the product of the row vector of the preparameter matrix and the postparameter

one. Substituting the modified second derivative into formula (1), the general dynamics model of an AV can be rewritten as

$$\bar{C}(q)\dot{\eta}+\bar{B}(q,\dot{q})\eta+\bar{F}+\bar{d}(t)=\bar{\tau}. \tag{3}$$

To overcome the shortcomings of pure kinematic controllers, several approaches have been proposed based on the integration of kinematic and dynamic models.

The following is a set of properties of the system (3) [28]:

- *Property 1*: $\bar{C}(q)$ and $\bar{B}(q,\dot{q})$ are bounded.
- *Property 2*: $\dot{\bar{C}}(q)-2\bar{B}(q,\dot{q})$ is skew symmetric.

To facilitate the control design and subsequent analysis, the dynamic model is transformed into

$$\dot{\eta}=M\eta+N\bar{\tau}+D, \tag{4}$$

where $N=\bar{C}^{-1}(q)$, $M=-\bar{C}^{-1}(q)\bar{B}(q,\dot{q})$, and $D=-\bar{C}^{-1}(q)(\bar{F}+\bar{d}(t))$. Note that the lumped disturbance D involves the unknown friction and external disturbance. To proceed, we introduce the following assumptions and lemmas.

Lemma 1

For a Gauss's hypergeometric function,

$$\mathbb{P}(\psi_1,\psi_2,\psi_3,\psi_4)=\sum_{k=0}^{\infty}\frac{(\psi_1)_k(\psi_2)_k}{(\psi_3)_k k!}\psi_4^k,$$

as long as ψ_1, ψ_2, $\psi_3\in\mathbb{R}^+$, $\psi_1+\psi_2<\psi_3$, and $\mathbb{P}(\cdot)$ will converge to a defined region $\psi_4<0$.

Lemma 2

Suppose that a positive–definite function $V(t)$ satisfies [31]

$$\dot{V}(t)+\kappa_1 V(t)+\kappa_2 V^{\kappa_3}(t)\le 0,\quad \forall t>T_0,$$

where $\kappa_1>0,\kappa_2>0$, and $0<\kappa_3<1$. Then, $V(t)$ can converge to zero in finite time T; that is,

$$T\le T_0+\frac{1}{\kappa_1(1-\kappa_3)}\ln\left[1+\frac{\kappa_1 V^{1-\kappa_3}(T_0)}{\kappa_2}\right],$$

where T_0 represents the initial time.

Lemma 3

Suppose $a_1>0,a_2>0,\ldots,a_n>0$, and $0<p<2$. The following inequality holds [32]:

$$(a_1^2+a_2^2+\cdots+a_n^2)^p\le(a_1^p+a_2^p+\cdots+a_n^p)^2.$$

Assumption 1

The lumped disturbance is bounded; i.e., $\|D\|\le\epsilon$, where ϵ represents an unknown positive constant.

Remark 1

Compared to the result [33] that D and $\dot{D}$ are bounded or that $\dot{D}$ is required to be vanishing, one needs to know only that the lumped disturbance is bounded. Also, the precise upper bound ϖ is not required in advance, while this point is essential in [34] and [35].

FLS

In this article, we design a fuzzy logic controller to attenuate the effect of the lumped disturbance. The fuzzy inference engine uses a fuzzy if-then rule to perform a mapping from an input vector $Z=[z_1,\ldots,z_n]^T\in\mathbb{R}^n$ to an output vector $W=[w_1,\ldots,w_n]^T\in\mathbb{R}^n$. The fuzzy linguistic rule base about the membership function of z_i and w_i is described in the following:

1) If z_i is a positive input (PI), w_i is a positive output (PO).
2) If z_i is a zero input (ZI), w_i is a zero output (ZO).
3) If z_i is a negative input (NI), w_i is a negative output (NO).

To satisfy the system performance requirements, the output signal of the FLS is designed as follows:

$$w_i=\frac{\sum_{j=1}^{3}m_j r_{ij}}{\sum_{j=1}^{3}m_j}=m_1r_{i1}+m_2r_{i2}+m_3r_{i3}, \tag{5}$$

Table 1. The investigated AV system's symbols.

Symbol	Description
OXY	Generalized coordinate system
$GX'Y'$	Vehicle body coordinate system
(x,y,θ)	Actual posture of the AV
v, w	Forward linear velocity and angular velocity
r, b, d	Radius of all wheels, distance between the driving wheel and the geometric midpoint C, and distance between the centroid point G and the geometric midpoint C
$q,\dot{q},\ddot{q}$	Generalized coordinates for the vehicle platform, velocity, and acceleration
$A(q), B(q,\dot{q})$ $E(q), F(\dot{q})C(q)$	Constraint vector, centripetal, Coriolis matrix, control coefficient matrix, unknown friction forces vector, and symmetric positive–definite inertia matrix
d,λ,τ	External disturbance, Lagrange multiplier, and control input

With the development of control theory and the growing demand for the finite-time tracking of vehicle systems, the finite-time controller has become a major research area.

where $0 \le m_j \le 1$ and $j = 1,2,3$ are the firing strengths of the ith rule; $r_a = [r_{a1}, r_{a2}, r_{a3}]^T \in \mathbb{R}^3$ signifies a fuzzy vector that must be properly chosen; $r_{i1} = -r_{ai}$, $r_{i2} = 0$, and $r_{i3} = r_{ai}$ indicate the center of the membership functions PO, ZO, and NO, respectively; and the relation $m_1 + m_2 + m_3 = 1$ is valid, according to the special condition of triangular membership functions.

From Figure 2, four possible cases appear in the following:

1) Only rule 1 is satisfied (that is, $z_i > z_a, m_1 = 1$, and $m_2 = m_3 = 0$); it follows that $w_i = r_{ai}$.
2) Both rule 1 and rule 2 are satisfied (that is, $0 < z_i \le z_a, 0 < m_1, m_2 \le 1$, and $m_3 = 0$); it follows that $w_i = m_1 r_{i1} = m_1 r_{ai}$.
3) Both rule 2 and rule 3 are satisfied (that is, $z_b < z_i \le 0, m_1 = 0$, and $0 < m_2, m_3 \le 1$); it follows that $w_i = m_3 r_{i3} = -m_3 r_{ai}$.
4) Only rule 4 is satisfied (that is, $z_i \le z_b, m_1 = m_2 = 0$, and $m_3 = 1$); it follows that $w_i = -r_{ai}$.

Recalling the aforementioned conditions, it we can obtain $z_i(m_1 - m_3) = |z_i(m_1 - m_3)| \ge 0$. In summary, we have

$$w_i = r_{ai}(m_1 - m_3). \tag{6}$$

Controller Design

Kinematic Controller Design for AVs

First, let us assume that an AV is expected to follow a trajectory with position $p_d = [x_d, y_d, \theta_d]^T$. Then, we can describe the trajectory equation as follows [36], [37]:

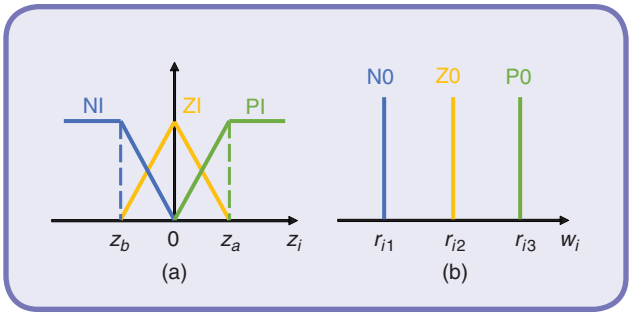

FIG 2 The membership functions. (a) The input fuzzy sets for z_i. (b) The output fuzzy sets for w_i.

$$\dot{p}_d = \begin{bmatrix} \dot{x}_d \\ \dot{y}_d \\ \dot{\theta}_d \end{bmatrix} = \begin{bmatrix} v_d \cos\theta_d \\ v_d \sin\theta_d \\ w_d \end{bmatrix} = \begin{bmatrix} \cos\theta_d & 0 \\ \sin\theta_d & 0 \\ 0 & 1 \end{bmatrix} \eta_d, \tag{7}$$

where $\eta_d = [v_d, w_d]^T$ represents the desired velocity signal, with v_d and w_d being the desired linear velocity and the desired angular velocity, respectively. Similarly, the actual trajectory of the AV can be described as

$$\dot{p} = \begin{bmatrix} \dot{x} \\ \dot{y} \\ \dot{\theta} \end{bmatrix} = \begin{bmatrix} v\cos\theta \\ v\sin\theta \\ w \end{bmatrix} = \begin{bmatrix} \cos\theta & 0 \\ \sin\theta & 0 \\ 0 & 1 \end{bmatrix} \eta, \tag{8}$$

where $p = [x, y, \theta]^T$ represents the actual motion trajectory of the AV and $\eta = [v, w]^T$ is the actual velocity vector, with v and w being the linear velocity and the angular velocity, respectively. The simple discrete-time kinematic can be written as

$$p_{t+\Delta t} = p_t + \Delta t \cdot \begin{bmatrix} \cos\theta_t & 0 \\ \sin\theta_t & 0 \\ 0 & 1 \end{bmatrix} \eta_t. \tag{9}$$

Inspired by [38] and [39], the posture error $p_e = (e_x, e_y, e_\theta)^T$ between p_d and p can be obtained as follows:

$$p_e = T_p(p_d - p), \tag{10}$$

where T_p represents the coordinate transformation matrix defined as

$$T_p = \begin{bmatrix} \cos\theta & \sin\theta & 0 \\ -\sin\theta & \cos\theta & 0 \\ 0 & 0 & 1 \end{bmatrix}. \tag{11}$$

Taking the time derivative of (10) yields

$$\dot{p}_e = \begin{bmatrix} \dot{e}_x \\ \dot{e}_x \\ \dot{e}_\theta \end{bmatrix} = \begin{bmatrix} \cos e_\theta & 0 \\ \sin e_\theta & 0 \\ 0 & 1 \end{bmatrix} \eta_d + \begin{bmatrix} -1 & e_y \\ 0 & -e_x \\ 0 & -1 \end{bmatrix} \eta. \tag{12}$$

In view of the Lyapunov theorem, an auxiliary kinematic control law applying the backstepping technique is designed as

$$\eta_c = \begin{bmatrix} v_c \\ w_c \end{bmatrix} = \begin{bmatrix} v_r \cos e_\theta + k_1 e_x \\ w_r + k_2 v_r e_y + k_3 v_r \sin e_\theta \end{bmatrix}, \tag{13}$$

where k_1, k_2, and k_3 are positive control gains to be designed and $v_r > 0$. More details are available in [40] and [41]. The objective of the following section is to develop control torque so that the overall system can achieve fast finite-time error convergence and chattering elimination despite the presence of lumped disturbances and actuator saturation.

SAFNFTSMC Design

First, the tracking error is defined as

$$\eta_e = \eta - \eta_c. \tag{14}$$

By substituting (14) into (4), the corresponding dynamics equation can be reorganized as

$$\dot{\eta}_e = M\eta_e - \dot{\eta}_c + M\eta_c + D + N\bar{\tau}. \tag{15}$$

For the purpose of fast finite-time error convergence, singularity avoidance, and robustness, the NFTSM manifold is developed in the form of [20], [21]

$$s = e + \gamma_1 \operatorname{sign}(e)^{\beta} + \gamma_2 \operatorname{sign}(\dot{e})^{\frac{l}{p}}. \tag{16}$$

Equation (16) represents the NFTSM sliding mode surface, so parameter s represents the sliding mode surface parament. Based on the goal of quickly reaching equilibrium along a given manifold, the control quantity is designed: $\gamma_1 > 0, \gamma_2 > 0, e = \int_0^t \eta_e(\zeta)\, d\zeta, \gamma_1 = \operatorname{diag}\{\gamma_{11}, \ldots, \gamma_{1n}\} \in \mathbb{R}^{n\times n}$, and $\gamma_2 = \operatorname{diag}\{\gamma_{21}, \ldots, \gamma_{2n}\} \in \mathbb{R}^{n\times n}$ are positive definite matrices. The parameters of l and p are both positive odd integers, which are required to hold the requirements that $1 < l/p < 2$ and $\beta > l/p$.

Subsequently, the complete torque controller is designed with consideration of the lumped disturbance:

$$\bar{\tau}_{sw} = N^{-1}(\bar{\tau}_{eq} + \bar{\tau}_{sw,1} + \bar{\tau}_{sw,2}), \tag{17}$$

with

$$\begin{aligned}
\bar{\tau}_{eq} &= -\frac{1}{\gamma_2}\frac{p}{l}\left(\operatorname{sign}(\dot{e})^{2-\frac{l}{p}} + \gamma_1\beta\,|e|^{\beta-1}\operatorname{sign}(\dot{e})^{2-\frac{l}{p}}\right) \\
&\quad - M\eta_e + \dot{\eta}_c - M\dot{\eta}_c, \\
\bar{\tau}_{sw,1} &= -k_a s + k_b \operatorname{sign}(s)^{\frac{k_c}{k_d}}, \\
\bar{\tau}_{sw,2} &= -r_a(m_1 - m_3),
\end{aligned}$$

where $\bar{\tau}_{eq}$ represents the equivalent controller, $\bar{\tau}_{sw,1}$ indicates the continuous FTSM-type control signal to guarantee fast finite-time error convergence and the elimination of chattering phenomenon, $k_a = \operatorname{diag}(k_{a1}, \ldots, k_{an}) \in \mathbb{R}^{n\times n}$ and $k_b = \operatorname{diag}(k_{b1}, \ldots, k_{bn}) \in \mathbb{R}^{n\times n}$ are positive–definite matrices, k_c and k_d are positive odd integers satisfying $k_c < k_d$, $\bar{\tau}_{sw,2}$ denotes a fuzzy control signal to dominate the unknown lumped disturbance, and the definitions of c_1, c_3, and r_a are given in (6). Importantly, it should be noted that, owing to $1 < l/p < 2$, controller (17) does not have a negative power fractional. As a result, it gives singularity-free control.

To avoid the "explosion term" problem caused by the repeated differentiation η_c, we define a new state variable η_f and let η_c pass the first-order filter:

$$\lambda\dot{\eta}_f + \eta_f = \eta_c, \qquad \eta_f(0) = \eta_c(0), \tag{18}$$

where λ represents the filter-time constant. Consider the Lyapunov function candidate as

$$V_1(t) = \frac{1}{2}s^T s. \tag{19}$$

By using (16)–(18) and applying the fact that $s(m_1 - m_3) = |s(m_1 - m_3)|$, with s being the input vector of the FLS, the derivative of V_1 can be computed along the NFTSM manifold as

$$\begin{aligned}
\dot{V}_1(t) &= s^T\Big\{\dot{e} + \gamma_1\beta\,|e|^{\beta-1}\dot{e} + \gamma_2\frac{l}{p}|\dot{e}|^{\frac{l}{p}-1}\Big[-k_b\operatorname{sign}(s)^{\frac{k_c}{k_d}} - k_a s \\
&\quad + D - \frac{1}{\gamma_2}\frac{p}{l}\left(\operatorname{sign}(\dot{e})^{2-\frac{l}{p}} + \gamma_1\beta|e|^{\beta-1}\operatorname{sign}(\dot{e})^{2-\frac{l}{p}}\right) \\
&\quad - r(m_1 - m_3)\Big]\Big\} \\
&\le -\sum_{i=1}^{n} s_i^2\left(\gamma_2 k_a\frac{l}{p}|\dot{e}|^{\frac{l}{p}-1}\right)_i - \sum_{i=1}^{n}|s_i|^{\frac{k_c+k_d}{k_d}}\left(\gamma_2 k_b\frac{l}{p}|\dot{e}|^{\frac{l}{p}-1}\right)_i \\
&\quad - \sum_{i=1}^{n}|s_i(m_1 - m_3)|\left(\gamma_2\frac{l}{p}|\dot{e}|^{\frac{l}{p}-1}\right)_i(r_{ai} - \Psi),
\end{aligned} \tag{20}$$

where $\Psi = |\epsilon/(m_1 - m_3)|$. As long as the inequality

$$r_{ai} \ge \Psi \tag{21}$$

holds, the value of $\dot{V}_1(t)$ remains nonpositive. Therefore, the closed-loop system is asymptotically stable.

Although the controller can handle the lumped disturbance to some extent, there are two technical difficulties that make it unsuitable for practical application, as in the following:

1) *Selection of the control parameter*: Since the accurate upper bound of the lumped disturbance is hard to know in practice, a big r_a needs to be chosen to ensure system stability. However, it may lead to more control energy and even to actuator saturation. To tackle these issues, we design an adaptive algorithm to adjust the parameter r_a:

$$\dot{\hat{r}}_a = \gamma_2\frac{l}{p}|\dot{e}|^{\frac{l}{p}-1}\frac{s(m_1 - m_3)}{\omega}, \quad \hat{r}_a(0) \ge 0, \tag{22}$$

where $\hat{r}_a = [\hat{r}_{a1}, \ldots, \hat{r}_{an}] \in \mathbb{R}^n$ and ω represents a positive constant determining the rate of the estimated bound $\hat{r}_a$. See the "Stability Analysis" section for a detailed proof.

2) *The problem of actuator saturation*: Since actuator saturation is a practical concern, consider the dynamics model given in (7), with actuator constraints as

$$\dot{\eta} = M\eta + Nu + D, \tag{23}$$

where u is the actual control input, designed as

$$u_i = \begin{cases} \bar{\tau}_{ri\max}\operatorname{sign}(\bar{\tau}_i), & |\bar{\tau}_i| \ge \bar{\tau}_{ri\max} \\ \bar{\tau}_i, & |\bar{\tau}_i| < \bar{\tau}_{ri\max} \end{cases}, \tag{24}$$

where $\bar{\tau} = [\bar{\tau}_1, \ldots, \bar{\tau}_n]^T \in \mathbb{R}^n$ represents the input of the saturation operation and $\bar{\tau}_{ri\max} > 0$ represents the saturation bound of the control input. To handle the influence on actuator saturation, an auxiliary system is constructed according to

$$\dot{\xi} = \begin{cases} -\alpha_1 \xi - \alpha_2 \xi^{\frac{a_3}{a_4}} - \dfrac{s^T s + \Delta u^T \Delta u}{2 \| \xi \|^2} \xi + \Delta u & \| \xi \| \geq \varsigma \\ 0 & \| \xi \| < \varsigma \end{cases}, \quad (25)$$

where $\Delta u = \bar{\tau} - u$, $\xi \in \mathbb{R}^n$ denotes the auxiliary term; $\alpha_1 = \mathrm{diag}(\alpha_{11}, \ldots, \alpha_{1n}) \in \mathbb{R}^{n \times n}$ and $\alpha_2 = \mathrm{diag}(\alpha_{21}, \ldots, \alpha_{2n}) \in \mathbb{R}^{n \times n}$ are positive–definite matrices; α_3 and α_4 are both positive odd integers, with $\alpha_3 < \alpha_4$; and ς is a small positive constant. Based on the previous analysis and synthesis, the SAFNFTSMC scheme is designed as

$$\begin{aligned} \bar{\tau} = N^{-1} \Big\{ & -\frac{1}{\gamma_2} \frac{p}{l} \Big(\mathrm{sign}(\dot{e})^{2-\frac{l}{p}} + \gamma_1 \beta |e|^{\beta - 1} \mathrm{sign}(\dot{e})^{2-\frac{l}{p}} \Big) \\ & - M \eta_e + \dot{\eta}_f - M \dot{\eta}_f + k_a s + k_b \mathrm{sign}(s)^{\frac{k_c}{k_d}} \\ & + \hat{r}_a (m_1 - m_3) + \xi \Big\}. \end{aligned} \quad (26)$$

A block diagram of the AV control system is in Figure 3.

Stability Analysis

Theorem 1

Consider an AV with respect to the lumped disturbance and actuator saturation (23), the described NFTSM manifold (16), and Assumption 1. Under the SAFNFTSMC scheme proposed in (18), (25), and (26), the tracking error will converge to zero in finite time.

Proof

The following proof is straightforward and constructive. Consider the Lyapunov function candidate as

$$V_2 = V_1 + \frac{\omega}{2} \sum_{i=1}^{n} \tilde{r}_{ai}^2 + \frac{1}{2} \xi^T \xi, \quad (27)$$

where $\tilde{r}_{ai} = \hat{r}_{ai} - \bar{r}_a$ and $\bar{r}_a$ represents an upper bound of $\hat{r}_{ai}$. Without the loss of generality, $\bar{r}_a$ is supposed to be $\bar{r}_a > \Psi + r_0$, and the parameter r_0 is a very small positive constant.

Condition 1

If $\| \xi \| \geq \varsigma$, where ς is a small positive constant, taking the time derivative of V_2 and applying the inequalities

$$s^T \xi \leq \frac{1}{2}(s^T s + \xi^T \xi), \quad \xi^T \Delta u \leq \frac{1}{2}(\xi^T \xi + \Delta u^T \Delta u) \quad (28)$$

yields

$$\begin{aligned} \dot{V}_2 &= s^T \gamma_2 \frac{l}{p} |\dot{e}|^{\frac{l}{p}-1} \Big(-k_a s - \mathrm{sign}(s)^{\frac{k_c}{k_d}} \Big) \\ &\quad - s^T \gamma_2 \frac{l}{p} |\dot{e}|^{\frac{l}{p}-1} (\hat{r}_a (m_1 - m_3) + D) + \omega \sum_{i=1}^{n} \tilde{r}_{ai} \dot{\hat{r}}_{ai} + \xi \dot{\xi} \\ &\leq s^T \gamma_2 \frac{l}{p} |\dot{e}|^{\frac{l}{p}-1} \Big(-k_a s - k_b \mathrm{sign}(s)^{\frac{k_c}{k_d}} \Big) \\ &\quad - s^T \gamma_2 \frac{l}{p} |\dot{e}|^{\frac{l}{p}-1} (\hat{r}_a (m_1 - m_3) + D) + \omega \sum_{i=1}^{n} \tilde{r}_{ai} \dot{\hat{r}}_{ai} \\ &\quad - \alpha_1 \xi^T \xi - \alpha_2 \xi^{\frac{\alpha_3 + \alpha_4}{\alpha_4}} - \frac{1}{2} s^T s - \frac{1}{2} \Delta u^T \Delta u + \xi^T \Delta u. \end{aligned} \quad (29)$$

On the premise of ensuring that the inequality of formula (29) does not change, the modified formula is scaled by adding and subtracting a term $s^T \gamma_2 \frac{l}{p} |\dot{e}|^{\frac{l}{p}-1} \bar{r}_a (m_1 - m_3)$ to the right-hand side of inequality (29), based on (22); then, the ideal goal of $\dot{V}_2 \leq 0$ is obtained:

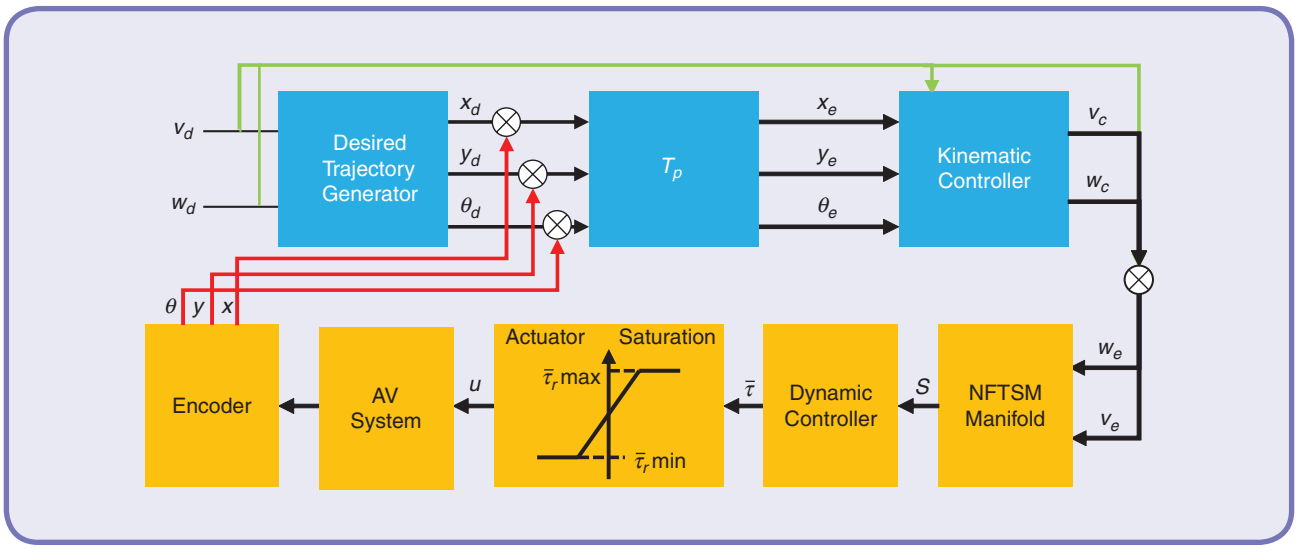

FIG 3 The control architecture.

$$
\begin{aligned}
\dot{V}_2 \le\ & s^T\gamma_2\frac{l}{p}|\dot{e}|^{\frac{l}{p}-1}\left(-k_a s-k_b\,\mathrm{sign}(s)^{\frac{k_c}{k_d}}\right)\\
& -s^T\gamma_2\frac{l}{p}|\dot{e}|^{\frac{l}{p}-1}\tilde{r}_a(m_1-m_3)-(\alpha_1-1)\xi^T\xi-\alpha_2\xi^{\frac{\alpha_3+\alpha_4}{\alpha_4}}\\
& +\sum_{i=1}^{n}\tilde{r}_{ai}s_i(m_1-m_3)\left(\gamma_2\frac{l}{p}|\dot{e}|^{\frac{l}{p}-1}\right)_i\\
& -s^T\gamma_2\frac{l}{p}|\dot{e}|^{\frac{l}{p}-1}(m_1-m_3)(\tilde{r}_a-\Psi)\\
\le & -\sum_{i=1}^{n}s_i^2\left(\gamma_2 k_a\frac{l}{p}|\dot{e}|^{\frac{l}{p}-1}\right)_i-\sum_{i=1}^{n}|s_i|^{\frac{k_c+k_d}{k_d}}\left(\gamma_2 k_b\frac{l}{p}|\dot{e}|^{\frac{l}{p}-1}\right)_i\\
& -\sum_{i=1}^{n}|s_i(m_1-m_3)|\left(\gamma_2\frac{l}{p}|\dot{e}|^{\frac{l}{p}-1}\right)_i\cdot r_0\\
& -(\alpha_1-1)\xi^T\xi-\alpha_2\xi^{\frac{\alpha_3+\alpha_4}{\alpha_4}}\\
\le & -\sum_{i=1}^{n}s_i^2\left(\gamma_2 k_a\frac{l}{p}|\dot{e}|^{\frac{l}{p}-1}\right)_i-\sum_{i=1}^{n}|s_i|^{\frac{k_c+k_d}{k_d}}\left(\gamma_2 k_b\frac{l}{p}|\dot{e}|^{\frac{l}{p}-1}\right)_i\\
& -(\alpha_1-1)\xi^T\xi-\alpha_2\xi^{\frac{\alpha_3+\alpha_4}{\alpha_4}}\le 0. \qquad (30)
\end{aligned}
$$

If $\alpha_1 > 1$, $\dot{V}_2$ will remain negative. Once the adaptive law estimates the unknown upper bound Ψ, it follows that $V_2 = V_1$. Since l and p are both positive odd integers satisfying $0 < l/p < 1$, there are two cases to be discussed.

Case 1

If $\dot{e} \neq 0$, it follows that $\gamma_2(l/p)|\dot{e}|^{\frac{l}{p}-1} > 0$ and $\dot{V}_2 < 0$. Therefore, the convergence property of the whole system can be guaranteed for $\dot{e} \neq 0$. Based on Lemma 3, we know that

$$
\dot{V}_2^* \le -2\Phi_1 V_2^* - 2^{\varrho}\Phi_2 V_2'^{*}, \qquad (31)
$$

in which $V_2^* = (1/2)s^T s + (1/2)\xi^T\xi$, $\varrho = \min\{((k_c+k_d)/2k_d), ((\alpha_3+\alpha_4)/2\alpha_4)\}$, $\Phi_1 = \min\{\pi_1, \alpha_1 - 1\}$, and $\Phi_2 = \min\{\pi_2, \alpha_2\}$, with π_1 and π_2 being the minimum eigenvalues of $\gamma_2 k_a(l/p)|\dot{e}|^{\frac{l}{p}-1}$ and $\gamma_2 k_b(l/p)|\dot{e}|^{\frac{l}{p}-1}$, respectively. With attention to $0 < (k_c+k_d)/2k_d < 1$ and Lemma 2, the NFTSM manifold can be found in finite time; namely,

$$
t_h \le t_0 + \frac{1}{2\Phi_1(1-\varrho)}\ln\left[\frac{\Phi_1(2V_2^*(t_0))^{1-\varrho}+\Phi_2}{\Phi_2}\right], \qquad (32)
$$

where $V_2^*(t_0)$ represents the condition at time t_0.

Case 2

If $\dot{e} = 0$, by substituting control input (29) into the vehicle system (26), we know that

$$
\ddot{e} = -k_a s - k_b\,\mathrm{sign}(s)^{\frac{k_c}{k_d}}. \qquad (33)
$$

For $s > 0$ and $s < 0$, it can be found that $\ddot{e} < 0$ and $\ddot{e} > 0$, respectively. Then, we know that $\ddot{e} = 0$ is not an attractor in the reaching phase and that the system state will not remain certain (i.e., $e = 0$ and $\dot{e} \neq 0$). Accordingly, the finite-time reachability of s can also be guaranteed for $\dot{e} = 0$.

Condition 2

If $\|\xi\| < \varsigma$ (i.e., $\dot{\xi} = 0$), there is no saturation constraint, and the corresponding proof is simpler than Condition 1. For brevity, detailed analyses are omitted. When the sliding surface $s = 0$ is reached, the following step is to discuss the convergence property of the NFTSM. Based on [42], the finite time t_{si} derived from $e(t_{di}) \neq 0$ to $e(t_{di}) + e(t_{si})$ can be computed according to

$$
t_{si} = \frac{\frac{l}{p}|e_i(t_{di})|^{1-\frac{p}{l}}}{\gamma_{1i}\left(\frac{l}{p}-1\right)}\cdot\mathbb{F}, \qquad (34)
$$

where $\mathbb{F} = \mathbb{P}((p/l), ((l/p)-1)/((\beta-1)(l/p)), 1+(((l/p)-1)/((\beta-1)(l/p))), -\gamma_1|e_i(t_{di})|^{\beta-1})$, $\mathbb{P}(\cdot)$ represents the Gauss's hypergeometric function [40], and the meaning of γ_{1i} is shown in formula (16). Due to $p < l$ and $\beta > 1$, it rapidly follows that $(p/l), ((l/p)-1)/((\beta-1)(l/p)), 1+(((l/p)-1)/((\beta-1)(l/p)))$, and $1+(((l/p)-1)/((\beta-1)(l/p))) - (p/l) > 0$. With attention to Lemma 1, $\mathbb{P}(\cdot)$ will have a convergent property. With this fact, the tracking error will converge to zero from any initial condition in finite time; namely, $t_s = \max\{t_{s1}, \ldots, t_{sn}\}$. In summary, the control objectives can be accomplished by the designed SAFNFTSMC. This completes the proof.

Remark 2

Because the sliding surface cannot remain exactly zero, it may have parameter drift. An efficient and simple solution is to turn off the parameter updating when the system state is smaller than a boundary value [31]. Thus, the adaption law is modified as follows:

$$
\dot{\hat{r}}_a = \begin{cases} \gamma_2\dfrac{l}{p}|\dot{e}|^{\frac{l}{p}-1}\dfrac{s(m_1-m_3)}{\omega}, & |\dot{e}| \neq \rho \\ 0, & |\dot{e}| \ge \rho \end{cases},
$$

where $\hat{r}_a(0) \ge 0$ and ρ is a small positive design parameter.

Experiment and Results

Setup

In this section, the differential drive Weihong AV is used to experimentally assess the designed control scheme, which is implemented via Visual C++ environments and runs on a personal computer with an Intel Core i5-7200V CPU at 2.5 GHz. The vehicle platform appears in Figure 4. The aluminum chassis of the vehicle is 82 × 82 × 30 cm and includes two driving wheels, two supporting wheels for balance, a laser range finder (Chuhang ARC1.01), a main control board, and a wireless communication device. Each wheel is driven by a dc motor (Maxon) and 48-V battery power. Each motor is mounted by the incremental encoder, and the gear reduction ratio is 80:1. Communication is achieved

through a controller area network bus. In addition, the posture of the AV is measured by an inertial navigation system (Huance CGI-410).

Extensive experiments with two tracking trajectories are performed to investigate the control performance of the proposed SAFNFTSMC method. To demonstrate feasibility and effectiveness, at 25 s, an extra 3-kg payload, as an external disturbance, is placed on the AV, away from the mass center. For comparison, tests of the FNFTSMC and the AFNFTSMC are performed. Here, only the SAFNFTSMC method can tackle the actuator saturation. For the sake of fairness, the controller parameters are chosen as $k_1 = 1, k_2 = 3, k_3 = 2, \gamma_{11} = \gamma_{12} = 0.75, \gamma_{21} = \gamma_{22} = 1.2$, $\beta = 2$, $l = 17$, $p = 13$, $k_a = k_b = 7$, $k_c = 6$, $k_d = 5$, and $\omega = 0.1$.

Results and Analysis

The results of the experiment are given in Figures 5–8. As shown in Figure 5, compared with the desired trajectory, the curve represented by the FNFTSMC has obvious fluctuation, especially at the corner. When changing the direction of the motion trajectory, the curve represented by the FNFTSMC cannot react quickly. Especially on the straight road section after turning, the curve represented by the FNFTSMC may deviate greatly from the desired trajectory. The proposed SAFNFTSMC method and the AFNFTSMC method have less deviation and a smaller curve fluctuation range than the desired trajectory. Therefore, the tracking performance of the AFNFTSMC and SAFNFTSMC methods is better than that of the FNFTSMC method. It should be noted that when the payload is suddenly increased, the

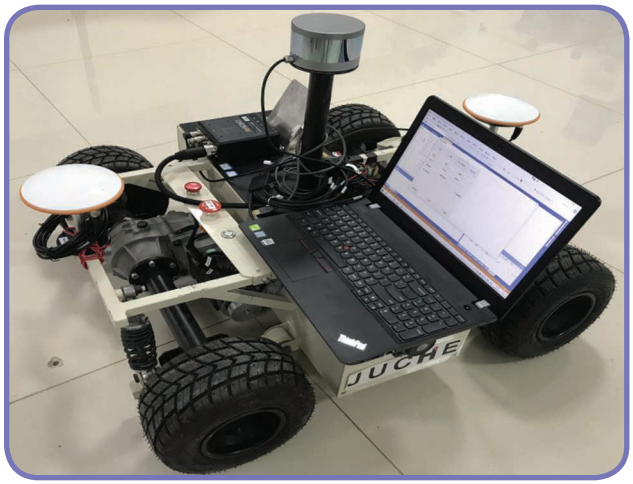

FIG 4 The AV platform.

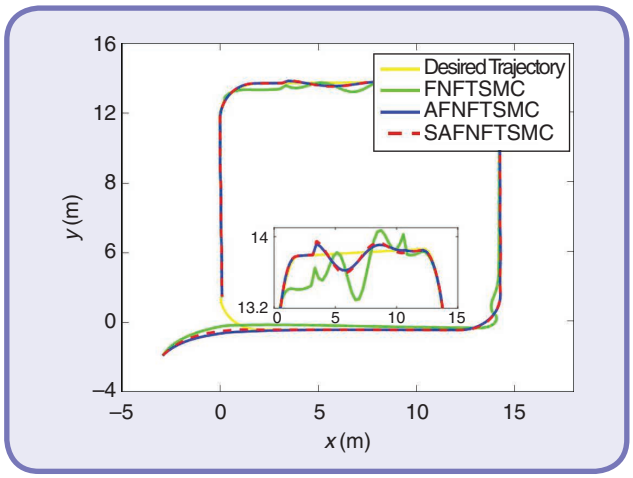

FIG 5 The tracking trajectory.

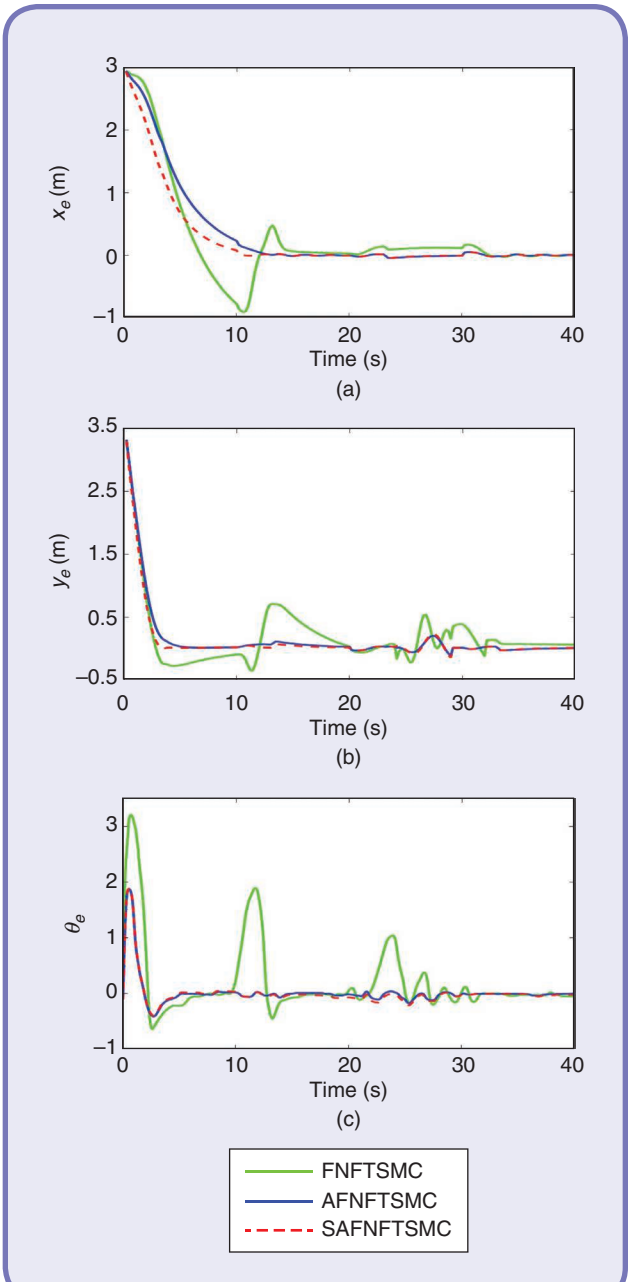

FIG 6 The tracking errors. (a) The *x*-axis. (b) The *y*-axis. (c) The directing angle θ.

proposed scheme can maintain superior tracking performance due to the adaptive algorithm.

According to the trajectory fluctuation, as presented in Figure 6, it is easy to see that the tracking performance of the FNFTSMC method is the worst among the three. The tracking error of the SAFNFTSMC is smaller than that of the AFNFTSMC, especially as shown in Figure 6(a), and the slope of the error curve of the SAFNFTSMC is larger than that of the AFNFTSMC in the initial stage, so the SAFNFTSMC has a faster tendency to reduce errors and achieve stability. It can still track the desired trajectory under both external disturbances and actuator saturation. Due to actuator saturation, the SAFNFTSMC needs some time to compensate for the lack of input torque. It is observed that the time to compensate for the input torque is very short, so it does not cause significant damage to the trajectory tracking process. This verifies that our designed control method has the ability to solve the problem of actuator saturation.

Figure 7 details the tracking error of the linear velocity and the angular velocity, and it can be seen that the AFNFTSMC and SAFNFTSMC methods have better transient performance. For example, when the given linear and angular velocities change suddenly in 10 s, the trajectory of the FNFTSMC fluctuates greatly in an instant and does not stabilize to an ideal value. Compared with the given linear and angular velocity curve, the AFNFTSMC and the SAFNFTSMC have less fluctuation, a smaller error, and more stability.

Furthermore, the input torque for the left and right wheels of the AV are plotted in Figure 8. It can be seen that the input torque of the FNFTSMC is the highest among the methods. This demonstrates that, due to the adaptive algorithm, the AFNFTSMC and SAFNFTSMC methods can avoid choosing a large control gain. Importantly, for the SAFNFTSMC method, the amplitude of the input torque is restricted to stay below the maximum torque, which is a result of the auxiliary system. The experiment results demonstrate that the AV can successfully track the desired trajectory despite the external disturbance and actuator saturation.

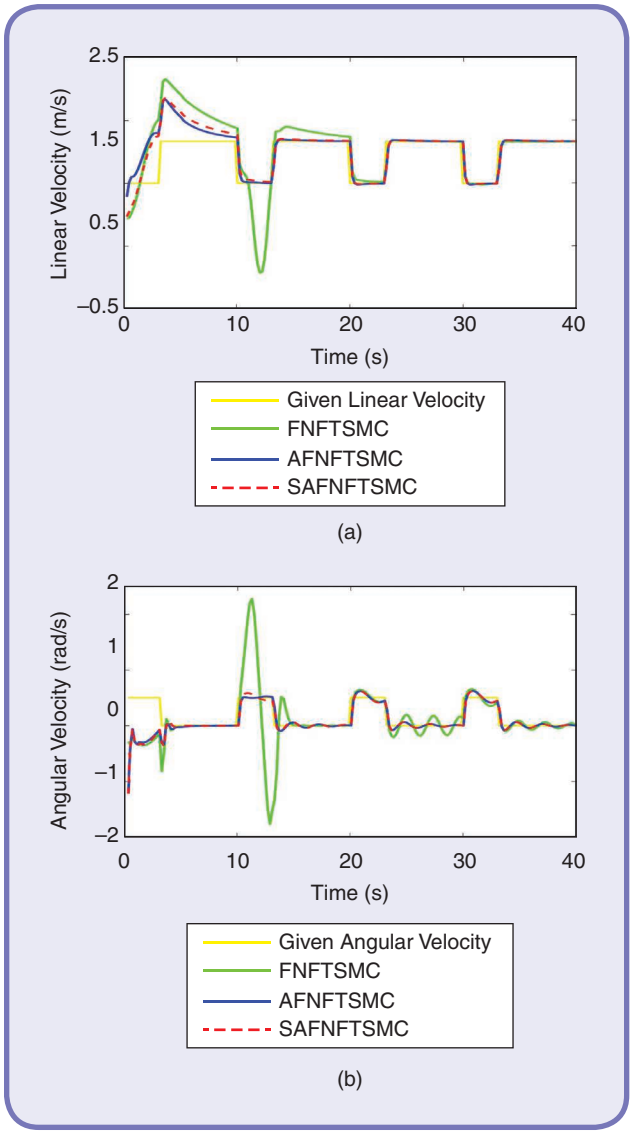

FIG 7 The velocity tracking. (a) The linear velocity. (b) The angular velocity.

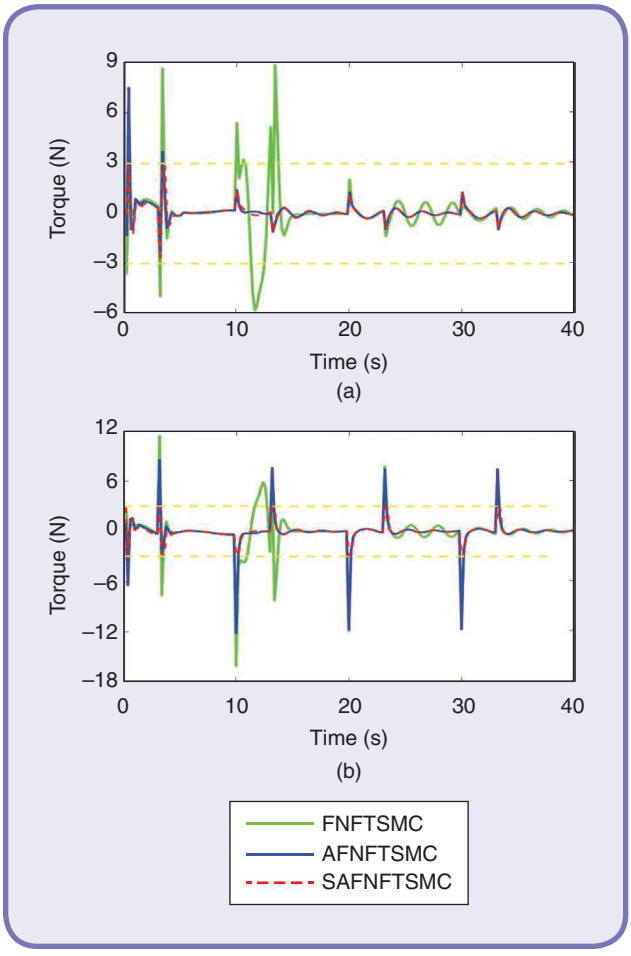

FIG 8 The torque. (a) The left wheel. (b) The right wheel.

Conclusion and Future Work

An adaptive finite-time trajectory tracking controller was designed for an AV, with an unknown lumped disturbance and actuator saturation, which is not only of practical interest but academically challenging. To handle the lumped disturbance, a fuzzy logic controller was designed. To guarantee the desired performance, including fast finite-time error convergence, chattering avoidance, and online gain adjustment, the AFNFTSMC scheme was proposed with the help of an adaptive mechanism and an NFTSM manifold. In addition, to attenuate the actuator constraint, an auxiliary system with a simple structure and only one tuning parameter was developed. Finally, experiment results demonstrated the effectiveness of the tracking controller. Future research will consider time delays and fault tolerance in AV control. Moreover, since not all system states are available in practice, additional work will consider a robust observer to estimate unmeasurable states.

Acknowledgments

This work was supported, in part, by the National Natural Science Foundation of China (grants U20A20225 and U2013601), Key Research and Development Plan of Anhui Province (grant 202004a05020058), Fundamental Research Funds for the Central Universities, Science and Technology Innovation Planning Project of the Ministry of Education of China, and NVIDIA AI Labs program. Experiments were conducted on a NVIDIA DGX-2.

About the Authors

Hongbo Gao (ghb48@ustc.edu.cn) earned his Ph.D. degree from Beihang University, Beijing, in 2016. He is an associate professor in the Department of Automation, School of Information Science and Technology, University of Science and Technology of China, Hefei, 230088, China. His research interests include unmanned system platforms and robotics, machine learning, decision support systems, and intelligent driving. He is the author or coauthor of more than 40 journal papers, and he is the coholder of 10 patent applications.

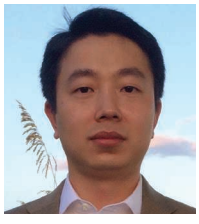

Zhen Kan (zkan@ustc.edu.cn) earned his Ph.D. degree, in 2011, from the Department of Mechanical and Aerospace Engineering, University of Florida, Gainesville. He is a professor in the Department of Automation, University of Science and Technology of China, Hefei, 230026, China. His research interests include networked robotic systems; Lyapunov-based nonlinear control; graph theory; complex networks; and human-assisted estimation, planning, and decision making.

Fei Chen (f.chen@ieee.org) earned his Dr. Eng. degree from the Fukuda Laboratory, Department of Micro–Nano Systems Engineering, Nagoya University, Japan, in 2012. He is an assistant professor and the leader of the Smart Manipulation Robots Laboratory, Department of Mechanical and Automation Engineering, T-Stone Robotics Institute, Chinese University of Hong Kong, Hong Kong, 999077, China. His research interests include robot learning, planning, and control for different formats of robot mobile manipulators.

Zhengyuan Hao (zyhao@mail.ustc.edu.cn) earned his B.S. degree in automation from Shandong University, Jinan, China, in 2019. He is pursuing his M.S. degree in control engineering at the University of Science and Technology of China, Hefei, 230026, China. His research interests include autonomous driving.

Xi He (hexi88@mail.ustc.edu.cn) earned her B.E. degree in automation from Hefei University of Technology, Anhui, China, in 2020. She is pursuing her M.S. degree in control engineering at the University of Science and Technology of China, Hefei, 230026, China. Her research interests include intelligent driving and environmental cognition.

Hang Su (hang.su@polimi.it) earned his Ph.D. degree in bioengineering, in 2019, from Politecnico di Milano, Milano, 20133, Italy, where he is a research fellow in the Department of Electronics, Information, and Bioengineering. His research interests include control and instrumentation in medical robotics, human–robot interaction, surgical robotics, deep learning, and bilateral teleoperation.

Keqiang Li (likq@tsinghua.edu.cn) earned his Ph.D. degree in automotive engineering from Chongqing University, China, in 1995. He is a professor of automotive engineering at the State Key Laboratory of Automotive Safety and Energy, Tsinghua University, Beijing, 100084, China. His research interests include vehicle dynamics, control for driver-assistance systems, and hybrid electrical vehicles. He has authored more than 90 papers and is a coholder of 12 patents in China and Japan.

References

[1] M. A. Kamel, X. Yu, and Y. Zhang, "Fault-tolerant cooperative control design of multiple wheeled mobile robots," *IEEE Trans. Control Syst. Technol.*, vol. 26, no. 2, pp. 756–764, Mar. 2018. doi: 10.1109/TCST.2017.2679066.

[2] S. L. Dai, S. He, X. Chen, and X. Jin, "Adaptive leader-follower formation control of nonholonomic mobile robots with prescribed transient and steady-state performance," *IEEE Trans. Ind. Inf.*, vol. 16, no. 6, pp. 3663–3671, June 2020.

[3] Y. Chen, Z. Li, H. Kong, and F. Ke, "Model predictive tracking control of nonholonomic mobile robots with coupled input constraints and unknown dynamics," *IEEE Trans. Ind. Inform*, vol. 15, no. 6, pp. 3196–3205, June 2019. doi: 10.1109/TII.2018.2874182.

[4] S. Rudra, R. K. Barai, and M. Maitra, "Design and implementation of a block-backstepping based tracking control for nonholonomic wheeled mobile robot," *Int. J. Robust Nonlinear Control*, vol. 26, no. 14, pp. 3018–3035, Sept. 2016. doi: 10.1002/rnc.3485.

[5] W. Sun, S. Tang, H. Gao, and J. Zhao, "Two time-scale tracking control of nonholonomic wheeled mobile robots," *IEEE Trans. Control Syst. Technol.*, vol. 24, no. 6, pp. 2059–2069, Nov. 2016. doi: 10.1109/TCST.2016.2519282.

[6] Z. P. Jiang and H. Nijmeijer, "Tracking control of mobile robots: A case study in backstepping," *Automatica*, vol. 33, no. 7, pp. 1393–1399, July 1997. doi: 10.1016/S0005-1098(97)00055-1.

[7] G. Oriolo, A. De Luca, and M. Vendittelli, "WMR control via dynamic feedback linearization: Design, implementation and experimental validation," *IEEE Trans. Control. Syst. Technol.*, vol. 10, no. 6, pp. 835–852, Nov. 2002. doi: 10.1109/TCST.2002.804116.

[8] D. Buccieri, D. Perritaz, P. Mullhaupt, Z.-P. Jiang, and D. Bonvin, "Velocity-scheduling control for a unicycle mobile robot: Theory and experiments," *IEEE Trans. Robot.*, vol. 25, no. 2, pp. 451–458, Apr. 2009. doi: 10.1109/TRO.2009.2014494.

[9] B. S. Park, J. B. Park, and Y. H. Choi, "Adaptive formation control of electrically driven nonholonomic mobile robots with limited information," *IEEE Trans. Syst., Man, Cybern. B*, vol. 41, no. 4, pp. 1061–1075, Aug. 2011.

[10] H. Gao et al., "Situational assessment for intelligent vehicles based on stochastic model and Gaussian distributions in typical traffic scenarios," *IEEE Trans. Syst. Man Cybern., Syst.*, early access, Sept. 18, 2020. doi: 10.1109/TSMC.2020.3019512.

[11] S. Xu, Y. Ou, J. Duan, X. Wu, W. Feng, and M. Liu, "Robot trajectory tracking control using learning from demonstration method," *Neurocomputing*, vol. 338, pp. 249–261, Apr. 2019. doi: 10.1016/j.neucom.2019.01.052.

[12] C.-L. Hwang, C.-C. Yang, and J. Y. Hung, "Path tracking of an autonomous ground vehicle with different payloads by hierarchical improved fuzzy dynamic sliding-mode control," *IEEE Trans. Fuzzy Syst.*, vol. 26, no. 2, pp. 899–914, Apr. 2018. doi: 10.1109/TFUZZ.2017.2698370.

[13] C. Fu, A. Sarabakha, E. Kayacan, C. Wagner, R. John, and J. M. Garibaldi, "Input uncertainty sensitivity enhanced nonsingleton fuzzy logic controllers for long-term navigation of quadrotor UAVs," *IEEE/ASME Trans. Mechatron.*, vol. 23, no. 2, pp. 725–734, Apr. 2018. doi: 10.1109/TMECH.2018.2810947.

[14] H. Du, G. Wen, Y. Cheng, Y. He, and R. Jia, "Distributed finite-time cooperative control of multiple high-order nonholonomic mobile robots," *IEEE Trans. Neural Netw. Learn. Syst.*, vol. 28, no. 12, pp. 2998–3006, Dec. 2017. doi: 10.1109/TNNLS.2016.2610140.

[15] S. Kamal, J. A. Moreno, A. Chalanga, B. Bandyopadhyay, and L. M. Fridman, "Continuous terminal sliding-mode controller," *Automatica*, vol. 69, pp. 725–734, July 2016. doi: 10.1016/j.automatica.2016.02.001.

[16] N. Wang, S. Lv, W. Zhang, Z. Liu, and M. J. Er, "Finite-time observer based accurate tracking control of a marine vehicle with complex unknown," *Ocean Eng.*, vol. 145, pp. 406–415, Nov. 2017. doi: 10.1016/j.oceaneng.2017.09.062.

[17] N. Wang, C. Qian, and Z.-Y. Sun, "Global asymptotic output tracking of nonlinear second-order systems with power integrators," *Automatica*, vol. 80, pp. 156–161, June 2017. doi: 10.1016/j.automatica.2017.02.026.

[18] D. Li, S. Ge, and H. Tong, "Simultaneous-arrival-to-origin convergence: Sliding-mode control through the norm-normalized sign function," *IEEE Trans. Autom. Control*, early access, Mar. 30, 2021. doi: 10.1109/TAC.2021.3069816.

[19] S. Li, H. Du, and X. Yu, "Discrete-time terminal sliding mode control systems based on Euler's discretization," *IEEE Trans. Autom. Control*, vol. 59, no. 2, pp. 546–552, Feb. 2014. doi: 10.1109/TAC.2013.2273267.

[20] J. Li, H. Du, Y. Cheng, X. Chen, and C. Jiang "Position tracking control for permanent magnet linear motor via fast nonsingular terminal sliding mode control," *Nonlinear Dyn.*, vol. 97, no. 4, pp. 2595–2605, Sept. 2019. doi: 10.1007/s11071-019-05150-y.

[21] M. Labbadi and M. Cherkaoui, "Robust adaptive nonsingular fast terminal sliding-mode tracking control for an uncertain quadrotor UAV subjected to disturbances," *ISA Trans.*, vol. 99, pp. 290–304, Apr. 2020. doi: 10.1016/j.isatra.2019.10.012.

[22] H. Taghavifar and S. Rakheja, "A novel terramechanics-based path-tracking control of terrain-based wheeled robot vehicle with matched-mismatched uncertainties," *IEEE Trans. Veh. Technol.*, vol. 69, no. 1, pp. 67–77, Jan. 2020. doi: 10.1109/TVT.2019.2950288.

[23] L. Zhou, Z. Che, and C. Yang, "Disturbance observer-based integral sliding mode control for singularly perturbed systems with mismatched disturbances," *IEEE Access*, vol. 6, pp. 9854–9861, Feb. 2018. doi: 10.1109/ACCESS.2018.2808477.

[24] N. Wang and Z. Deng, "Finite-time fault estimator-based fault-tolerance control for a surface vehicle with input saturations," *IEEE Trans. Ind. Inform*, vol. 16, no. 2, pp. 1172–1181, July 2019.

[25] Z. Liu, Z. Han, Z. Zhao, and W. He, "Modeling and adaptive control for a spatial flexible spacecraft with unknown actuator failures," *Sci. China Inf. Sci.*, vol. 64, p. 152,208, Apr. 2021. doi: 10.1007/s11432-020-3109-x.

[26] N. Sun, T. Yang, and Y. Fang, "Transportation control of double pendulum cranes with a nonlinear quasi-PID scheme: Design and experiments," *IEEE Trans. Syst. Man Cybern. Syst.*, vol. 49, no. 7, pp. 1408–1418, July 2019. doi: 10.1109/TSMC.2018.2871627.

[27] M. Chen, G. Tao, and B. Jiang, "Dynamic surface control using neural networks for a class of uncertain nonlinear systems with input saturation," *IEEE Trans. Neural Netw. Learn. Syst.*, vol. 26, no. 9, pp. 2086–2097, Sept. 2015. doi: 10.1109/TNNLS.2014.2360933.

[28] H. Yang, X. Fan, P. Shi, and C. Hua, "Nonlinear control for tracking and obstacle avoidance of a wheeled mobile robot with nonholonomic constraint," *IEEE Trans. Control Syst. Technol.*, vol. 24, no. 2, pp. 741–746, Mar. 2016.

[29] C. Lian, X. Xu, H. Chen, and H. He, "Near-optimal tracking control of mobile robots via receding-horizon dual heuristic programming," *IEEE Trans. Cybern.*, vol. 46, no. 11, pp. 2484–2496, Nov. 2016. doi: 10.1109/TCYB.2015.2478857.

[30] M. Abramowitz and I. A. Steegun, *Handbook of Mathematical Functions: With Formulas, Graphs, and Mathematical Tables*. New York: Dover, 1972.

[31] S. Yu, X. Yu, B. Shirinzadeh, and Z. Man, "Continuous finite-time control for robotic manipulators with terminal sliding mode," *Automatica*, vol. 41, no. 11, pp. 1957–1964, Nov. 2005. doi: 10.1016/j.automatica.2005.07.001.

[32] S. He, D. Lin, and J. Wang, "Autonomous spacecraft rendezvous with finite time convergence," *J. Franklin Inst.*, vol. 352, no. 11, pp. 4962–4979, Nov. 2015. doi: 10.1016/j.jfranklin.2015.08.008.

[33] S. Shi, X. Yu, and S. Khoo, "Robust finite-time tracking control of nonholonomic mobile robots without velocity measurements," *Int. J. Control*, vol. 89, no. 2, pp. 411–423, Feb. 2016. doi: 10.1080/00207179.2015.1079735.

[34] V. Men, H. J. Kang, and K. S. Shin, "Novel quasi-continuous super-twisting high-order sliding mode controllers for output feedback tracking control of robot manipulators," *Proc. Inst. Mech. Eng. C—J. Eng. Mech. Eng. Sci.*, vol. 228, no. 17, pp. 3240–3257, Dec. 2014. doi: 10.1177/0954406214526828.

[35] L. Zhang, L. Liu, Z. Wang, and Y. Xia, "Continuous finite-time control for uncertain robot manipulators with integral sliding mode," *IET Contr. Theory Appl.*, vol. 12, no. 11, pp. 1621–1627, July 2018. doi: 10.1049/iet-cta.2017.1361.

[36] A. Liu, W.-A. Zhang, M. Z. Q. Chen, and L. Yu, "Moving horizon estimation for mobile robots with multirate sampling," *IEEE Trans. Ind. Electron.*, vol. 64, no. 2, pp. 1457–1467, Feb. 2017. doi: 10.1109/TIE.2016.2611458.

[37] W. He, T. Meng, X. He, and S. Sam Ge, "Unified iterative learning control for flexible structures with input constraints," *Automatica*, vol. 96, pp. 326–336, Oct. 1, 2018. doi: 10.1016/j.automatica.2018.06.051.

[38] D. Li and H. Gao, "A hardware platform framework for an intelligent vehicle based on a driving brain," *Engineering*, vol. 4, no. 4, pp. 464–470, 2018. doi: 10.1016/j.eng.2018.07.015.

[39] X. Yu, W. He, H. Li, and J. Sun, "Adaptive fuzzy full-state and output feedback control for uncertain robots with output constraint," *IEEE Trans. Syst., Man, Cybern., Syst.*, early access, Feb. 3, 2020. doi: 10.1109/TSMC.2019.2963072.

[40] B. Paden, M. Cap, S. Z. Yong, D. Yershov, and E. Frazzoli, "A survey of motion planning and control techniques for self-driving urban vehicles," *IEEE Trans. Intell. Transp. Syst.*, vol. 1, no. 1, pp. 33–55, Mar. 2016. doi: 10.1109/TIV.2016.2578706.

[41] H. Gao, J. Zhu, X. Li, Y. Kang, J. Li, and H. Su, "Automatic parking control of unmanned vehicle based on switching control algorithm and backstepping," *IEEE/ASME Trans. Mechatron.*, early access, Nov. 10, 2020. doi: 10.1109/TMECH.2020.3037215.

[42] L. Yang and J. Yang, "Nonsingular fast terminal sliding-mode control for nonlinear dynamical systems," *Int. J. Robust Nonlinear Control*, vol. 21, no. 16, pp. 1865–1879, Nov. 2011. doi: 10.1002/rnc.1666.

ITS